Vol. 551: 117–130, 2016
doi: 10.3354/meps11703

MARINE ECOLOGY PROGRESS SERIES
Mar Ecol Prog Ser

Published June 9

Validation and improvement of species distribution models for structure-forming invertebrates in the eastern Bering Sea with an independent survey

Christopher N. Rooper[1,*], Michael F. Sigler[2], Pam Goddard[1], Pat Malecha[3], Rick Towler[1], Kresimir Williams[1], Rachel Wilborn[1], Mark Zimmermann[1]

[1]Resource Assessment and Conservation Engineering Division, Alaska Fisheries Science Center, Seattle, Washington 98115, USA
[2]Habitat and Ecological Processes Research Program, and [3]Auke Bay Laboratories, Alaska Fisheries Science Center, Juneau, Alaska 99801, USA

ABSTRACT: Species distribution modeling is a useful tool for informing ecosystems management. However, validation of model predictions through independent surveys is rarely attempted in marine environments, which are challenging to study and often contain sensitive habitats. We conducted an underwater camera survey of the eastern Bering Sea slope and outer shelf as an independent test of species distribution modeling of deep-sea corals, sponges and sea whips based on bottom trawl survey data. We also refined model predictions by combining species distribution models based on both bottom trawl and underwater camera survey data. The camera survey also was conducted to determine density and size of the taxa. The trawl model predictions generally were confirmed by the camera observations (area under the receiver–operator curve [AUC] values of 0.63 to 0.73). Combining bottom trawl and camera survey model predictions improved predictive ability (AUC values of 0.74 to 0.90 for camera observations). Corals were distributed in Pribilof Canyon and the slope area to the northwest of the canyon, and colony densities averaged 0.005 ind. m^{-2} and ranged from 0 to 0.28 ind. m^{-2}. The low densities were consistent with the absence of hard substrates for coral attachment in most areas of the eastern Bering Sea. Sponge and sea whip density averaged 0.11 ind. m^{-2}, with sponge density ranging from 0 to 13.1 and sea whip density ranging from 0 to 8.4 ind. m^{-2}. Invertebrate heights were generally small, with most taxonomic groups <20 cm in average height. This type of study is vital to providing the best scientific advice for spatial management of structure-forming invertebrates, so that decisions concerning the protection of these vulnerable communities can be implemented with a clear basis for priorities.

KEY WORDS: Benthic invertebrates · Habitat · Underwater survey · Species distribution models · Model validation · Invertebrate size structure · Density · Eastern Bering Sea · Alaska

INTRODUCTION

Species distribution models take many forms, but are generally spatially explicit models that predict the distribution of organisms using environmental or habitat factors as explanatory variables. They are increasingly used to develop spatial management plans in both terrestrial and marine environments. Common applications of species distribution models have been to protect habitat for endangered or rare species (Engler et al. 2004, Kumar & Stohlgren 2009), design spatial management plans (Guisan et al. 2013, Abecasis et al. 2014) and predict responses to future climate change (Wiens et al. 2009, Kaplan et al. 2016). In addition, species distribution modeling can inform fisheries management in marine environ-

*Corresponding author: chris.rooper@noaa.gov

ments where habitat features may be vulnerable to fishing gear impacts.

For sessile, vulnerable species such as deep-sea corals and sponges, species distribution models are often built on available data sources, such as historical records from museum specimens, interviews or other literature archives (Leverette & Metaxas 2005, Bryan & Metaxas 2007), commercial fishing bycatch (Taylor et al. 2013), fisheries stock assessment survey bycatch (Rooper et al. 2014), underwater image surveys (Woodby et al. 2009, Howell et al. 2011, Krigsman et al. 2012, Anderson et al. 2016), or combinations of many data sources with little underlying *a priori* survey design or disparate survey designs (Davies et al. 2008, Rengstorf et al. 2013, Guinotte & Davies 2014, Miller et al. 2015). These species distribution models may be useful for management, but their predictions are rarely verified with independent surveys.

On the eastern Bering Sea slope and outer shelf in Alaska, concern has been raised over the potential effects of commercial fishing on vulnerable benthic habitats, primarily deep-sea corals, in 2 large canyons along the slope: Pribilof and Zhemchug canyons (Miller et al. 2012, Sigler et al. 2015). The eastern Bering Sea slope and outer shelf is a region of enhanced primary and secondary productivity that attracts large numbers of fishes, seabirds and marine mammals (Springer et al. 1996). About 40% of U.S. commercial fisheries catch originates from the eastern Bering Sea (Voorhees & Lowther 2012), with some fisheries concentrated on the slope and outer shelf.

In response to these concerns, species distribution models were developed based on data from bottom trawl surveys (2002 to 2012); model predictions were expressed as the probability of presence for each taxonomic grouping on the eastern Bering Sea slope and outer shelf (Sigler et al. 2015). A key outcome of this distribution modeling was the finding that about 1/3 of the predicted coral habitat for the eastern Bering Sea slope occurs in Pribilof Canyon, an area that comprises only about 10% of the total slope area. Much of the remaining predicted coral habitat was found in the inter-canyon slope area to the northwest of Pribilof Canyon. However, it was unclear if the bottom trawl survey data used to develop these models were adequate to determine the distribution of deep-sea corals and other structure-forming invertebrates along the Bering Sea slope and outer shelf. For example, bottom trawling is difficult in high relief or hard seafloor areas, where one might expect to find structure-forming invertebrates.

Thus, the primary objective of this study was to evaluate previous species distribution models (Sigler et al. 2015) for deep-sea corals and other structure-forming invertebrates with an independent underwater camera survey. The secondary objectives were to use the new data to improve model predictions by model averaging and to determine the densities of structure-forming invertebrates where they occurred as well as their size.

MATERIALS AND METHODS

Study area

The eastern Bering Sea is dominated by a broad, shallow continental shelf that stretches east to west from the Alaska mainland to the shelf break roughly 700 km away (Fig. 1). The eastern Bering Sea shelf is commonly divided into the following 3 domains based on bathymetry and oceanographic fronts: the inner shelf (0 to 50 m), the middle shelf (50 to 100 m) and the outer shelf (100 to 180 m) (Coachman 1986). The shelf break is typically at 180 to 200 m depth, except at the northern edge of Bering Canyon, where the shelf break is at 500 m (Sigler et al. 2015). The eastern Bering Sea slope is made up of 5 major canyons (Bering, Pribilof, Zhemchug, Pervenets and Navarin canyons) with an inter-canyon area between each (Fig. 1). In addition to the 9 regions (canyon and inter-canyon) along the continental slope, this study also focuses on the outer shelf region of the eastern Bering Sea.

Survey design and field sampling

A total of 300 sampling station locations were randomly selected from a regular-spaced grid (100 × 100 m) overlaid on the eastern Bering Sea outer shelf and slope. Random stations were chosen so that each of the 9 slope areas received a minimum of 10 stations. The additional 210 stations were randomly chosen throughout the 9 slope areas and the outer shelf, in proportion to probability of coral presence from the bottom trawl model of coral distribution (Sigler et al. 2015). Thus, areas with a higher probability of coral presence (such as Pribilof Canyon, the adjacent inter-canyon area to the northwest, and the outer shelf near Pribilof Canyon and to the north and south) were allocated more stations (Fig. 1). Owing to poor weather and time constraints, only 250 of the 300 stations were occupied during field sampling

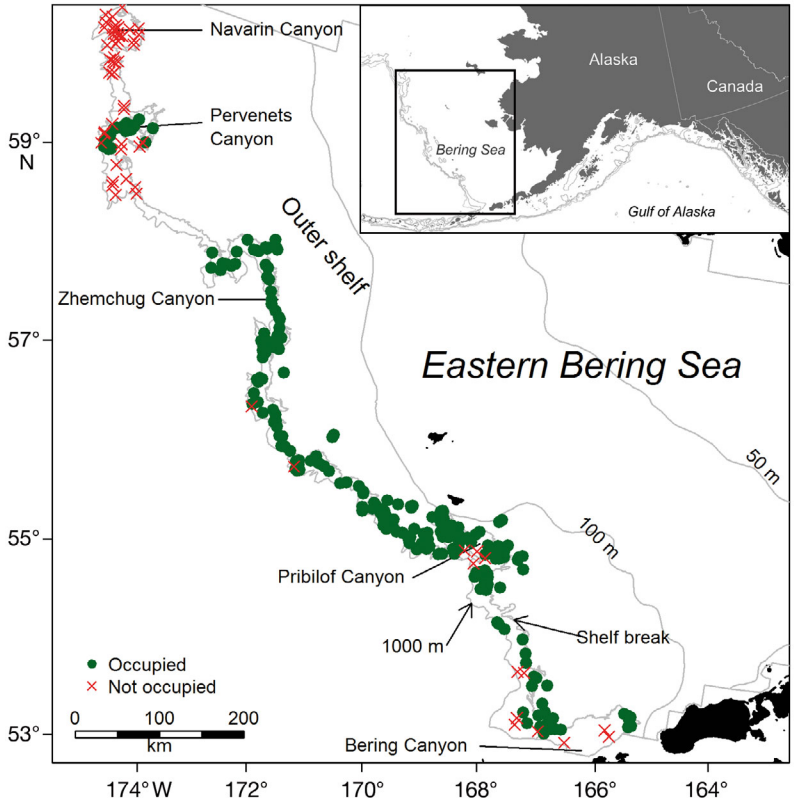

Fig. 1. Eastern Bering Sea slope and outer shelf. Map includes locations of the 5 major canyons and the inter-canyon areas. Randomly selected sample sites are indicated as occupied and those not sampled due to time or depth constraints. The 50, 100 and 1000 m isobaths are shown, as well as the shelf break designation. Map is shown in an Alaska Albers equal area conic projection

(Table 1), with the majority of unsampled stations north of Zhemchug Canyon (Fig. 1). The survey was conducted from 8 August to 6 September 2014.

The primary sampling tools for this study were 2 calibrated stereo drop-cameras deployed from a chartered fishing vessel (see Williams et al. 2010 and Supplement 1 at www.int-res.com/articles/suppl/m551p117_supp.pdf for details on these systems). At each station, the camera was deployed at the center of the grid cell and lowered to the seafloor. Once seafloor contact was made, the drop-camera was drifted or towed along the bottom for 15 min at a speed of 0.48 to 3.34 km h^{-1} (0.26 to 1.8 knots) in the direction of the prevailing current. The camera was held approximately 1 to 2 m above the substrate, with the cameras pointed slightly downward at an angle of approximately 35° off parallel to the seafloor. The position of the camera throughout the deployment was assumed to be the same as the research vessel GPS. The deployment cable was held as near vertical as possible to improve positional accuracy, given weather and wind conditions. The distances traveled during deployments ranged from 27 to 839 m (362 ± 8.8 m, mean ± SE). Only 4 tows were less than 100 m long and these were the result of equipment failure (such as dying batteries). Over 85% of the deployments sampled distances between 200 and 600 m.

Post-cruise image analysis was conducted to determine substrate types, species density and height. Image pairs collected during each deployment were viewed using stereo image processing software developed in the Python programming language (K. Williams unpubl. software). To compute range and size information, the cameras were calibrated to correct for image distortion due to the lens and viewport optics, and to solve for the epipolar geometry between the 2 cameras (Williams et al. 2010). The image analysis software then determined the 3-dimensional coordinates of corresponding points identified in stereo-image pairs using a stereo-triangulation function.

The substrate observed in the underwater video transects was classified by a commonly used seafloor substratum classification scheme (Stein et al. 1992, Yoklavich et al. 2000), which consists of a 2-letter coding of substratum type, denoting a primary sub-

Table 1. Summary of stations occupied in each area of the eastern Bering Sea slope and outer shelf. The total number of stations with each taxonomic group of structure-forming invertebrates is also given for each area

Area	Stations sampled	Corals	Sponges	Sea whips
Bering Canyon	10	0	5	3
Bering–Pribilof inter-canyon	17	0	4	9
Pribilof Canyon	36	18	24	9
Pribilof–Zhemchug inter-canyon	68	12	29	31
Zhemchug Canyon	25	1	12	11
Zhemchug–Pervenets inter-canyon	15	0	11	7
Pervenets Canyon	12	0	2	4
Outer shelf	67	1	26	31
Total	250	32	113	105

stratum with >50% coverage and a secondary substratum with 20 to 49% coverage of the seafloor. There were 8 identified substratum types: mud (M), sand (S), gravel–pebble (G, diameter <6.5 cm), mixed course material (MC), cobble (C, 6.5 < diameter < 25.5 cm), boulder (B, diameter >25.5 cm), exposed low relief bedrock (R) and exposed high relief bedrock (K). By this classification, a section of seafloor covered primarily in cobble, but with boulders over more than 20% of the surface, would receive the substratum code cobble–boulder (Cb) with the secondary substratum indicated by the lower-case letter. The substratum code was only changed if a substratum encompassed more than 10 sequential images. The size of each substrate was estimated from the viewing path width or by direct measurement.

All structure-forming invertebrates (corals, sponges and sea whips), fishes and crabs were identified to the lowest possible taxonomic level and counted for each transect. The lowest possible taxonomic level was typically genus for corals and sea whips, and order for sponges (Stone et al. 2011, Stone 2014, R. Stone, Alaska Fisheries Science Center, pers. comm.). Although sea whips (family Halipteridae) are in the subclass containing corals (Octocorallia), they were considered separately from other corals from the suborders Holaxonia (family Plexauridae) and Calcaxonia (families Primnoidae and Isididae), because the preference of sea whips for sandy, unconsolidated substrates differs from the preference of other corals for rocky substrate (cobble, boulder, or exposed bedrock). Careful examination and accounting of individual targets in adjacent frames ensured that objects were only counted once. Demosponges on 4 transects were too numerous to count individually, so 135 image pairs were randomly subsampled, and all of the individual sponges in these frames enumerated expanded to the unsampled frames. Sponges less than 10 cm in height were difficult to discern from other small white- or yellow-colored items on the seafloor, so these were not included in the counts or analyses.

Densities of individual taxa were calculated by di<viding transect counts by the area swept (distance observed × path width observed). The median range (in cm) of all objects counted on a transect was assumed to be the distance from the camera where 100% of fishes and invertebrates were detected for that transect. A swath width at the median range was calculated by combining the known viewing angle for each camera (fixed by the camera lens) and the median range to objects on a transect. The mean path width across all transects was 3.08 ± 0.05 m, with a minimum of 1.55 m and a maximum of 5.51 m for any individual transect. The area viewed on each transect ranged from 84 to 3441 m^2 and averaged 1131 ± 34 m^2.

Structure-forming invertebrate heights were obtained by triangulating the pixel coordinates of corresponding points (the base and the tip of the invertebrate) seen in the left and right camera frames. Heights of all corals where the base and tip could be observed were measured. Sea whip and sponge heights were measured for all individuals whose density was lower than ~500 on a transect. For transects with more than ~500 individual sea whips or sponges, a random subsample of ~200 heights were measured. Curved sea whips were measured to their highest point above the seafloor. Except where noted, the height data from each transect were weighted by the density of the taxa for that transect. Our calculations produced presence or absence, densities (no. m^{-2}) and heights of structure-forming invertebrates, and proportions of each type of substrate.

Validation and construction of presence–absence models

Distribution models of corals, sponges and sea whips for the eastern Bering Sea outer shelf and slope were originally developed from bottom trawl survey data from 2002 to 2012 (Sigler et al. 2015, details provided in Supplement 2). Validation was conducted by comparing the predictions of probability of structure-forming invertebrate presence from bottom trawl survey models to the observations of their presence or absence from the independent camera survey. The maximum probability of presence for each structure-forming invertebrate predicted by the bottom trawl survey model was extracted for each camera survey transect and compared to the camera observation of presence or absence at that site (see Supplement 2 for details).

Using only the camera survey data, a second set of generalized additive models (GAMs) was also developed to predict presence or absence of structure-forming invertebrates (Wood 2006). These models used some of the same explanatory variables (latitude, depth, bottom temperature, slope, mean current speed, maximum tidal current speed, ocean color, grain size and sediment sorting) as the bottom trawl survey model for its predictions (see Supplement 2 for details).

Predictions from the cross-validated bottom trawl survey model and the camera survey model were

averaged for each grid cell on the maps of the eastern Bering Sea slope and outer shelf. These averages were weighted by the inverse of the prediction error for each grid cell. The resulting map of predictions at each grid cell reflected the average predicted probability for the 2 models, and the confidence of that prediction (i.e. grid cells where the bottom-trawl-based model had a high prediction error were down-weighted relative to the camera-based model, where its prediction error was low). As the camera survey extended to a depth of only 808 m, and the trawl survey extended to 1200 m depth, the average predictions extended to a depth of only 825 m, where both models were supported by observations. The resulting average prediction was tested against the observations from the 2 surveys (bottom trawl and camera) using the standard set of diagnostics (area under the receiver–operator curve [AUC], correlation and percent correct).

Density and height distribution of structure-forming invertebrates

Hurdle models (Cragg 1971, Potts & Elith 2006) predicting the spatial distributions of density and height using the camera survey data were produced for each structure-forming invertebrate taxonomic grouping. Hurdle models predict the spatial distribution of density (or, in this case, density and height) in the following 3 stages: (1) probability of presence is predicted from presence–absence data using the average prediction for each taxonomic group developed in the previous section; (2) a threshold presence probability is determined using the optimum thresholds determined by the camera data; and (3) a separate model is constructed that predicts density (or height) using the density and height data from the camera survey. For each taxonomic grouping, the density or height of the species was predicted by a GAM model utilizing latitude, depth, bottom temperature, slope, mean current speed, maximum tidal current speed, ocean color and sediment size. In the GAM model estimation, only transects with non-zero values were included. Density data was fourth-root transformed to best meet the assumption of normality, whereas height was untransformed. Models of density and height were evaluated against observations using the deviance explained and correlations between observations and predictions. All the analyses, modeling and mapping were carried out using R software (R Development Core Team 2013)

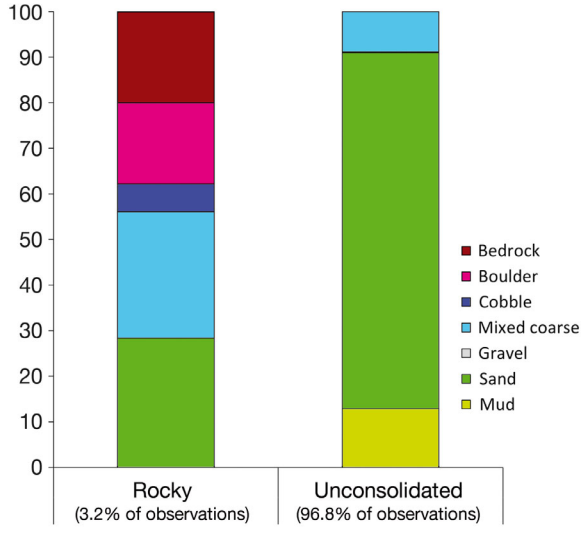

Fig. 2. Percentages of primary seafloor substrates observed during the camera survey. Substrates were divided into purely unconsolidated (containing only mud, sand, gravel or mixed coarse substrates; 96.8% of the total observations) and rocky (those containing any type of cobble, boulder or exposed bedrock; 3.2% of the total observations)

RESULTS

The 250 transects were located from Bering Canyon in the south to Pervenets Canyon in the north; the depths sampled ranged from 91 to 808 m, with a median of 276 m (Table 1, Fig. 1). Almost 97% of the images of the seafloor contained unconsolidated substrates (mud, sand, gravel, pebble or mixed coarse material), with sand as the dominant substrate observed (Fig. 2). The remaining 3.2% of images contained some type of rocky substrate (cobble, boulder or exposed bedrock); however, only 1.4% of the images had rocky substrates as the primary substrate type. Over 70000 structure-forming invertebrates were observed (Table 2). Most were demosponges (55%), predominantly from 2 individual transects, and sea whips (40%). Few were corals (2%, <1500 individuals).

Corals occurred at 32 transects and were classified into 5 taxonomic groups, including 3 families (Primnoidae, Plexauridae and Isididae) and 2 genera (*Plumarella* sp. and *Swiftia* sp.). Corals occurred at 50% of transects in Pribilof Canyon and about 18% of transects in the inter-canyon area between Pribilof and Zhemchug canyons. Coral was also present at 1 station on the outer shelf and 1 station in Zhemchug Canyon (Table 1, Fig. 3). Of the transects with coral, 11 had <5 individual colonies occurring on them. Sponges occurred on 113 transects and were classi-

Table 2. Summary of structure-forming invertebrate taxonomic groupings observed during the 2014 camera survey on the eastern Bering Sea slope and outer shelf. Also given are the mean, minimum and maximum depths at which each taxonomic grouping was observed

Taxonomic grouping	No. observed	Mean depth (m)	Min depth (m)	Max depth (m)
Demospongiae	37682	352	110	770
Halipteris spp.	29435	304	91	760
Hexactinellida	1952	395	110	770
Plumarella sp.	775	555	349	761
Swiftia sp.	537	546	264	770
Isididae	69	562	349	760
Primnoidae	38	492	212	760
Plumarella aleutiana	36	555	349	761
Calcarea	31	428	215	532
Unidentified sponges	27	553	150	761
Plexauridae	8	631	455	759
Unidentified corals	2	695	–	–

fied into 3 classes: Hexactinellida, Demospongiae and Calcarea (Table 2). Sponges were widely distributed and occurred in all of the sampled regions (Fig. 3), ranging from a low of 17% (2 out of 12) of the stations in Pervenets Canyon to a high of 73% (11 out of 15) of stations in the inter-canyon region between Zhemchug and Pervenets canyons (Table 1). Sea whips were also widely distributed both in terms of region (Table 1) and depth (Table 2).

Validation and construction of presence–absence models

The species distribution models based on bottom trawl survey data (Sigler et al 2015) predicted the presence or absence of structure-forming invertebrates in the camera survey very well. Over 72% of coral, 59% of sponge and 65% of sea whip camera observations were predicted correctly by the bottom trawl survey models (for details see Supplement 2 at www.int-res.com/articles/suppl/m551p117_supp.pdf). The best-fitting models of structure-forming invertebrate groups using only the camera survey data tended to be similar to those constructed using bottom trawl survey data for corals, but differed somewhat for sea whips and sponges (Supplement 2). The camera survey models correctly predicted 87% of the coral presence or absence observations from the camera survey, as well as 73% of the sponge and 76% of the sea whip observations. Likewise, the camera survey models effectively predicted the bottom trawl occurrences of coral (78% of cases), but were less accurate in predicting occurrences of sponges and sea whips (50% and 55%, respectively). The combined models (trawl plus camera) performed best, with 81% of coral, 71% of sponge and 70% of sea whip camera observations correctly predicted. The trawl model predictions generally were confirmed by the camera observations (AUC values of 0.63 to 0.73). Combining bottom trawl and camera survey model predictions improved predictive ability (AUC values of 0.74 to 0.90 for camera observations). The average predictions (combining predictions from the bottom trawl and camera survey models) showed relatively high probability of coral occurrence in Pribilof Canyon and the area to

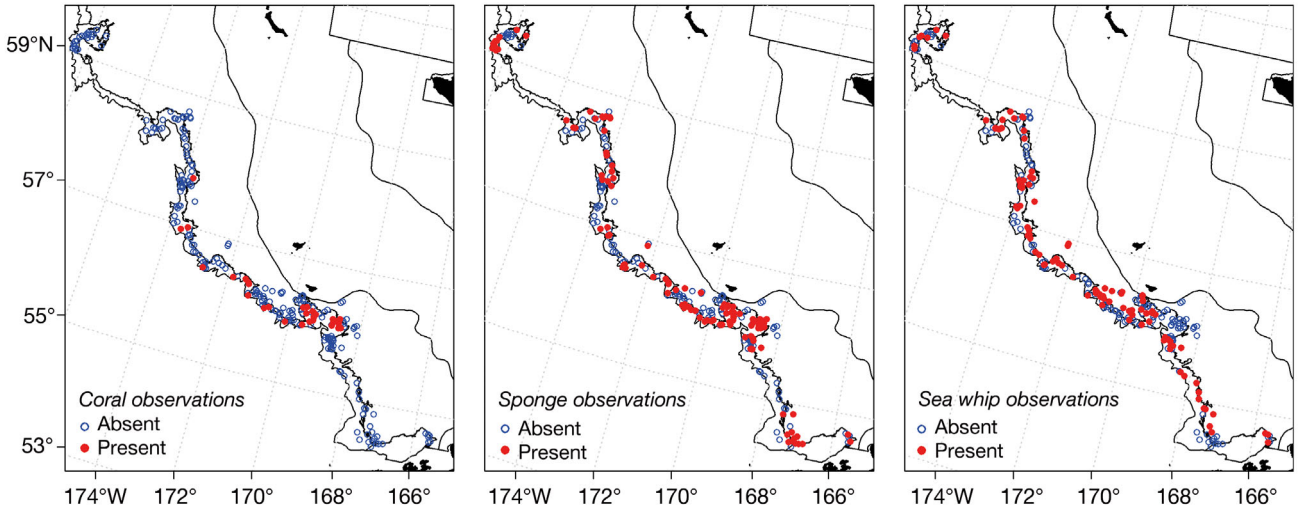

Fig. 3. Observations of presence or absence for each taxa of structure-forming invertebrates from the 2014 stereo camera survey on the eastern Bering Sea slope and outer shelf (n = 250)

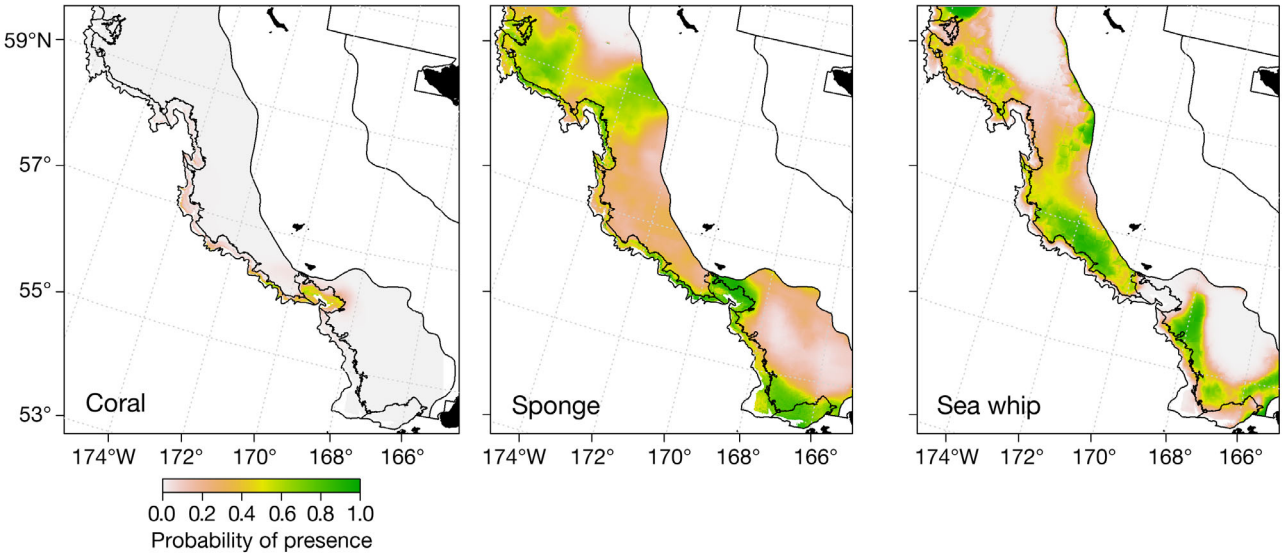

Fig. 4. Average probability of structure-forming invertebrate presence from the weighted predictions of the best-fitting generalized additive models of presence or absence from the trawl survey data and camera survey data. The predictions were averaged by weighting with the inverse of the prediction error. Panels represent coral, sponge and sea whip predictions on a 100 × 100 m grid

the northwest, high probability of sponge occurrence in Bering Canyon, Pribilof Canyon and the area to the northwest, Zhemchug Canyon and in areas of the outer shelf, and high probability of sea whip occurrence along the outer shelf and some in deeper waters (Fig. 4).

Density and height distribution of structure-forming invertebrates

The densities of coral at individual transects were very low (0.005 ± 0.002 ind. m^{-2}) and ranged from 0 to 0.28 ind. m^{-2}. The highest densities of coral were observed in Pribilof Canyon and to the northwest. The best-fitting GAM predicting coral density explained 70% of the variability (Table 3). Density increased with increasing depth and decreased with increasing slope (Fig. 5). Density of coral predicted by the model matched the observations, with highest densities in Pribilof Canyon and to the northwest in deeper waters (Fig. 6).

The densities of demosponge at transects averaged 0.11 ± 0.06 ind. m^{-2} and ranged from 0 to a high of 13.1 ind. m^{-2}. The average density of hexactinellid sponges was 0.006 ± 0.002 ind. m^{-2}. A total of 4 of the transects had densities of sponges in excess of 0.5 ind. m^{-2}; these transects all occurred in the middle region of the eastern Bering Sea slope and outer shelf from Pribilof Canyon to just north of Zhemchug

Table 3. Best-fitting generalized additive models (GAMs) predicting density and height of corals, sponges and sea whips using data from the 2014 camera survey of the eastern Bering Sea slope and outer shelf. Terms are listed in order of importance in the models; estimated degrees of freedom (edf) for each of the variables are also given

Response variable	GAM	Deviance explained (%)	edf	R^2
Coral density	s(slope) + s(depth)	70	2.3, 2.7	0.62
Sponge density	s(latitude) + s(grain size) + s(current speed)	20	2.3, 2.9, 1.0	0.13
Sea whip density	s(depth) + s(slope)	33	2.9, 2.6	0.28
Coral height	s(latitude) + s(tidal current) + s(slope) + s(grain size) + s(temperature) + s(current speed)	93	3.0, 1.0, 1.2, 1.8, 2.1, 2.6	0.86
Sponge height	s(temperature) + s(slope) + s(grain size)	41	2.0, 2.0, 2.6	0.36
Sea whip height	s(depth) + s(temperature) + s(latitude) + s(current speed) + s(grain size)	60	2.4, 2.7, 1.9, 1.0, 1.0	0.55

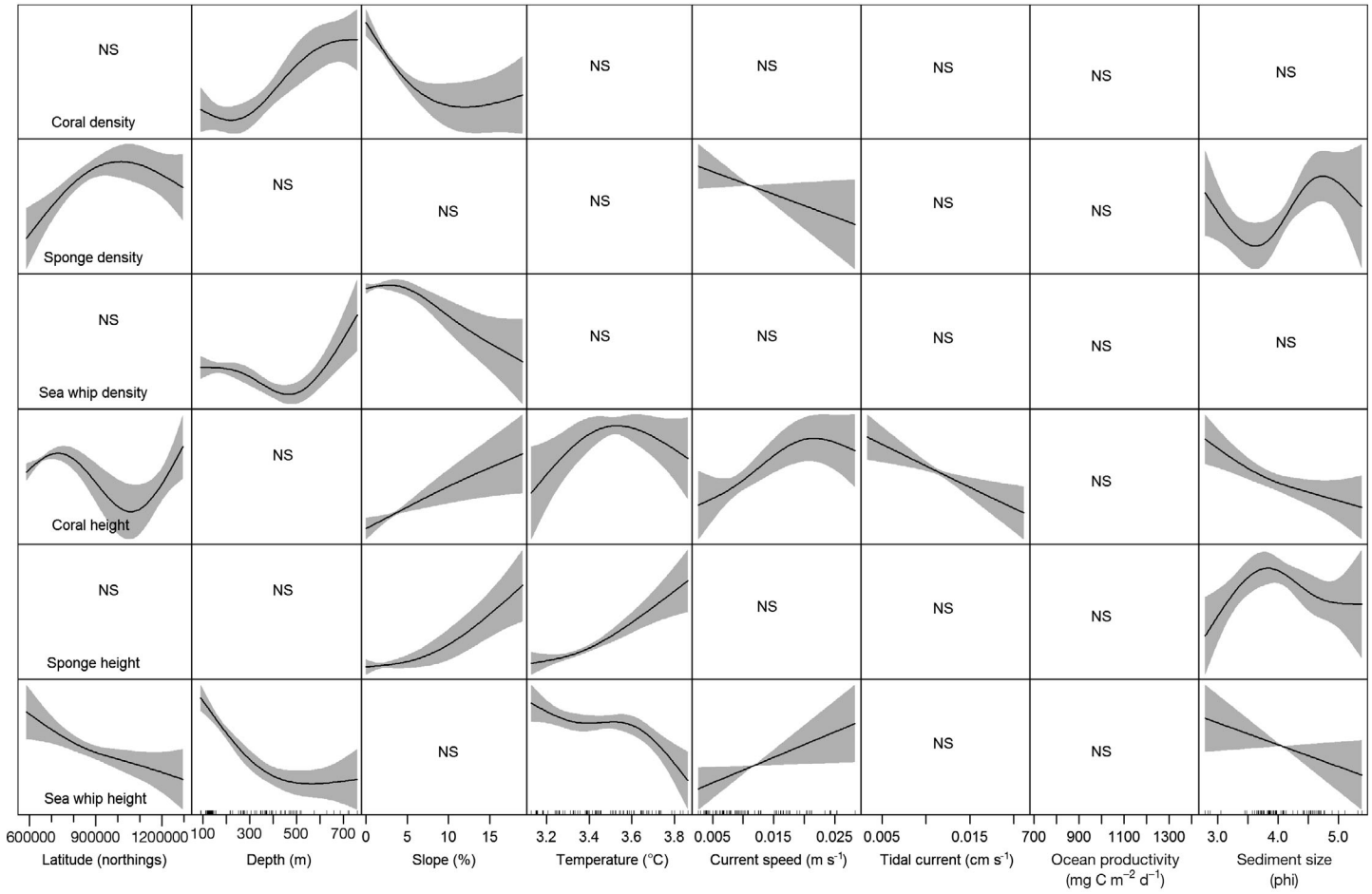

Fig. 5. Smoothed relationships from the best-fitting generalized additive model between explanatory variables and the density of corals, sponges and sea whips from the camera survey, and the heights measured for structure-forming invertebrates for the camera survey. NS: not significant

Canyon. The best-fitting GAM explained only 20% of the variability in the sponge densities (Table 3). Density decreased with increasing current speed, and sponge density was highest at the smallest grain sizes and at phi of ~4.5. However, this relationship may have reflected low sample sizes at some of the middle values of phi (Fig. 5). Density of sponge predicted by the model was highest in Pribilof Canyon and on the surrounding outer shelf (Fig. 6). Two large areas of predicted high density of sponge on the outer shelf northeast of Zhemchug Canyon and southeast of Pervenets Canyon were not sampled during the camera survey and likely are spurious.

The densities of sea whips found at transects averaged 0.11 ± 0.04 ind. m^{-2} and ranged from 0 to a high of 8.4 ind. m^{-2}. A total of 10 transects had densities of sea whips in excess of 0.5 ind. m^{-2}. The best-fitting GAM predicting sea whip density included only bottom depth and slope as significant factors, similar to the coral model (Table 3). The sea whip GAM explained 33% of the variability in the density data, but unlike the model of coral density, sea whip density decreased with increasing depth, except for an uptick in density at the deepest depths below 600 m (Fig. 5). Density of sea whips was predicted to be relatively uniform and high on the outer shelf and slope (Fig. 6).

The height of corals varied by taxonomic group (Table 4). On average, colonies from the family Isididae were the tallest, ranging from 10 to 116 cm, while *Swiftia* sp. were the shortest, ranging from 2 to 24 cm. Most corals were <20 cm in height (Table 4). Corals were largest on the slope northwest of Pribilof Canyon. The best-fitting GAM predicting coral height included latitude, maximum tidal current speed, slope, sediment grain size, temperature and average current speed as significant factors, and explained 93% of the data variability (Table 3). Gen-

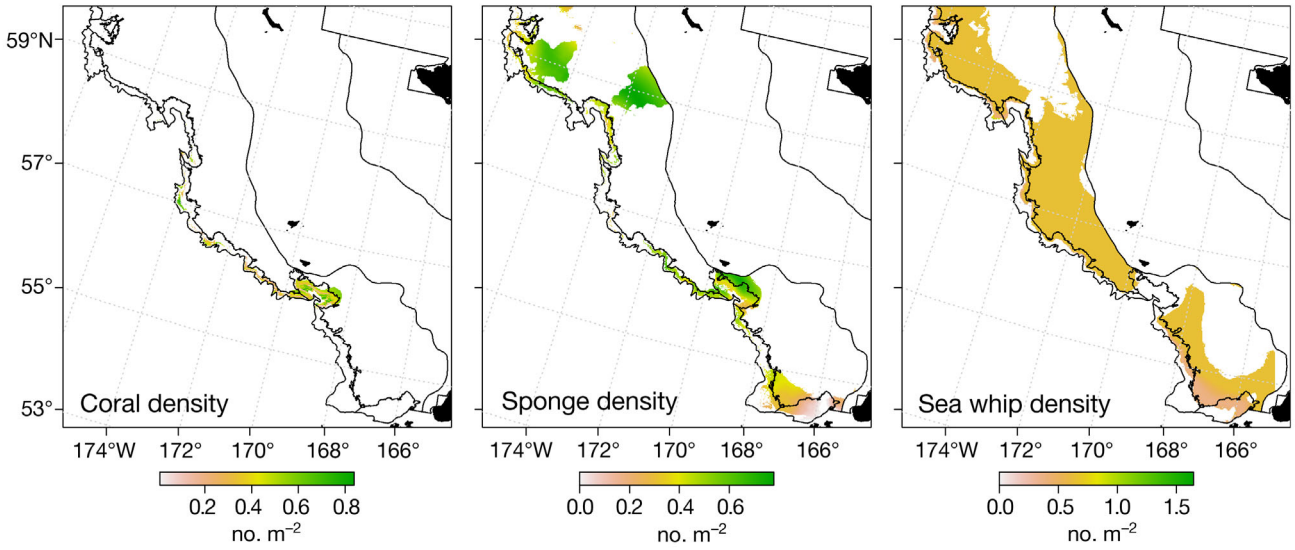

Fig. 6. Predicted fourth-root transformed density (no. m^{-2}) of corals, sponges and sea whips based on GAMS of camera survey density data. Predictions are shown for only those grid cells where the average presence–absence model indicated that the invertebrate taxa would be present

erally, coral height increased with increasing slope, and corals were tallest in deeper waters between Pribilof Canyon and Zhemchug Canyon (Fig. 5). Interestingly, coral heights increased with increasing average current speed, but decreased strongly with increasing tidal current speed.

Sponges across all groups averaged about 17 cm (range 13 to 25 cm) in height (Fig. 7). However, sponges <10 cm in height were not measured or counted, so this average is biased high. Hexactinellid sponges tended to be the largest, with 1 specimen having a height of >2 m (Table 4). Sponges were tallest at or near the shelf break around Bering Canyon, Pribilof Canyon and to the northwest of Pribilof Canyon. The best-fitting GAM predicting sponge height included temperature, slope and sediment grain size as significant factors (Table 3). The model explained 41% of the variability in the data, and heights increased with increasing slope and temperature, and peaked at a phi of about 3.5 (corresponding to fine sand to very fine sand) (Fig. 5). Sponges were predicted to be tallest in Bering Canyon and on the outer shelf area to the north, and around Pribilof Canyon and deeper waters to the northwest (Fig. 8).

Table 4. Average heights for invertebrate taxa measured during the eastern Bering Sea slope and outer shelf camera survey. The number measured (n), mean, standard deviation (SD), minimum and maximum heights are given (cm)

Species	n	Mean	SD	Min	Max
Gorgonacea	2	21	9.2	15	28
Isididae	31	48	28.4	10	116
Plexauridae	1	16		16	16
Plumarella aleutiana	4	12	7.2	6	22
Plumarella sp.	265	16	9.4	4	53
Primnoidae	19	11	8.3	4	33
Swiftia sp.	41	10	4.2	2	24
Porifera	3	17	4.4	13	22
Calcarea	12	13	2.0	10	18
Demospongiae	1972	18	8.3	10	135
Hexactinellida	569	25	18.5	10	204
Halipteris spp.	3496	62	54.2	2	266

Sea whips exhibited a bimodal height frequency (Fig. 7), with many individuals <40 cm tall, but with another peak in height at about 110 cm. On a few occasions, sea whip heights were measured at >2 m as well. The largest sea whips were observed between Pribilof Canyon and Zhemchug Canyon at or near the shelf break. The best-fitting GAM predicting sea whip height included depth, temperature, latitude, average current speed and sediment grain size as significant factors, and explained 60% of the variability in the data (Table 3). Sea whip height decreased with increasing depth, temperature and sediment size (Fig. 5). Sea whip height also decreased from south to north. Current speed was the only factor that had a positive effect on sea whip height. Sea whips were tallest in the outer shelf region between Pribilof and Zhemchug canyons (Fig. 8).

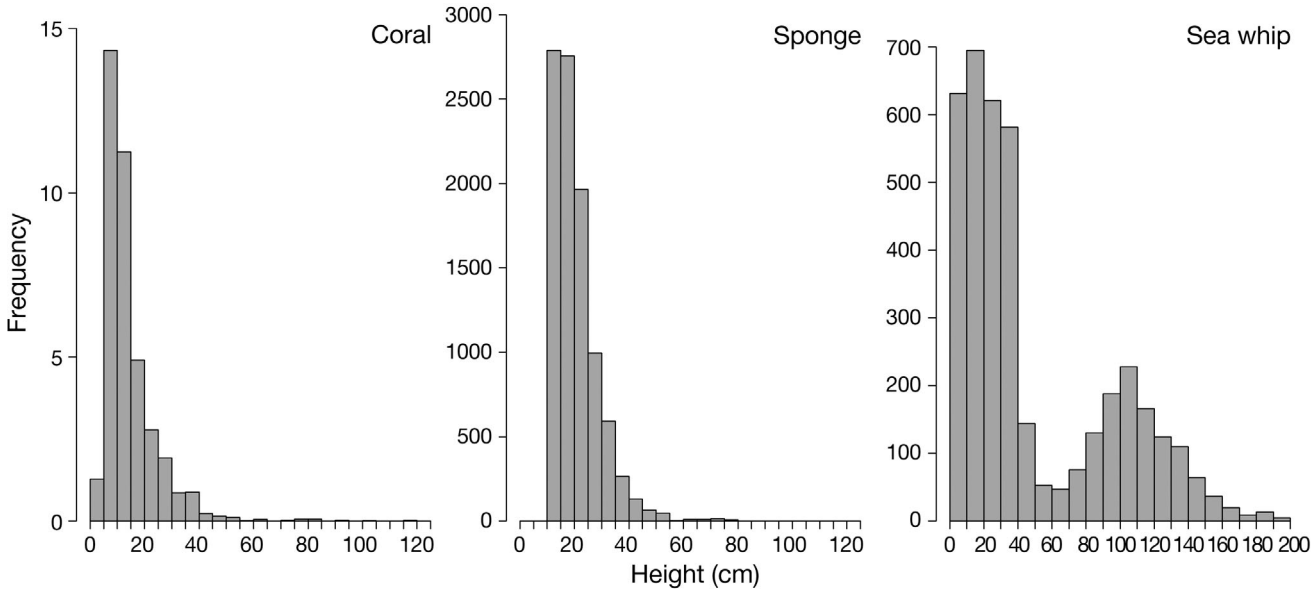

Fig. 7. Height frequencies measured by the stereo camera for invertebrate taxa: corals, sponges and sea whips

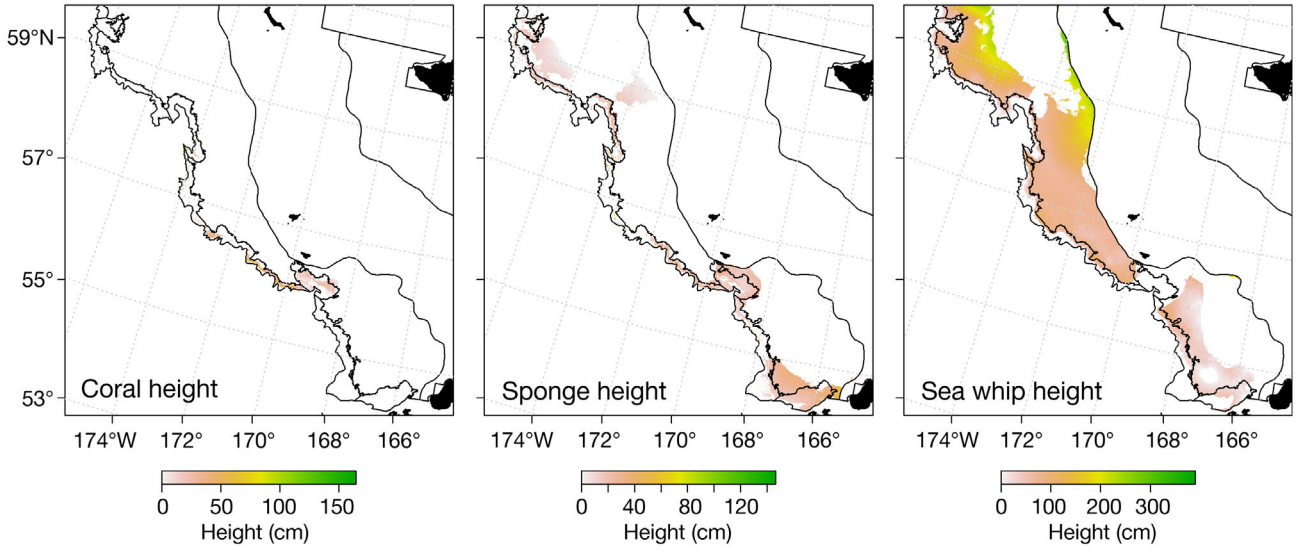

Fig. 8. Predicted heights of corals, sponges and sea whips based on GAM models of camera survey density data. Predictions are shown for only those grid cells where the average presence–absence model indicated that the invertebrate taxa would be present

DISCUSSION

Coral and sponge distribution

The density of coral found in this study (0.005 ind. m^{-2}) was lower than previous studies focused on Pribilof and Zhemchug canyons. Previous density estimates for gorgonian corals were 0.73 ± 0.04 ind. m^{-2} in Pribilof Canyon and 0.13 ± 0.1 ind. m^{-2} in Zhemchug Canyon (Miller et al. 2012). In the Miller et al. (2012) study, transects were placed systematically in presumed coral habitat rather than randomly, and their sample size was low (16 transects), which probably accounts for most of the differences in coral density. In addition, some transects were clustered so that only 9 distinct geographic locations were sampled (5 within or near Zhemchug Canyon and 4 within or near Pribilof Canyon), rather than the nominal sample size of 16 transects (Miller et al. 2012). In contrast, we sampled 25 locations within

Zhemchug Canyon and 36 locations within Pribilof Canyon.

The density of corals that we found for the eastern Bering Sea was much less than densities found elsewhere in Alaska. In the central Aleutian Islands, Stone (2006) estimated an average coral density of 1.23 ind. m^{-2} and a maximum density of 3.85 ind. m^{-2}. In the Gulf of Alaska, a study of Primnoa thickets yielded densities of red tree coral of 0.52 ind. m^{-2} (Stone 2014). Coral densities differ among the regions of Alaska because of differences in the amount of appropriate substrates available for colonization. Since corals require hard substrate for attachment, most are found in areas with exposed rocky substrate; we found that rocky substrates were limited in the eastern Bering Sea.

Sponges were distributed more broadly than corals, with most sponges found on the outer shelf and slope regions from Bering Canyon to just northwest of Pribilof Canyon, where they were the most dense. The density of sponges for the eastern Bering Sea averaged 0.11 ind. m^{-2}. In comparison, sponge densities averaged 2.51 ind. m^{-2} in the Gulf of Alaska (Stone 2014); in Pribilof and Zhemchug canyons, hexactinellid densities averaged 0.40 and 0.02 ind. m^{-2}, respectively, and other sponges (likely demosponges) averaged 0.24 and 0.001 ind. m^{-2} (Miller et al. 2012). Sponges were fairly ubiquitous and were found over a wide range of substrate types and depths in this and the other studies. This is likely a function of the low taxonomic resolution applied to the group.

The camera survey indicated that sea whips were distributed on the outer shelf to both the north and south of Pribilof Canyon, with the tallest and most dense sea whips found to the north of Pribilof Canyon on the outer shelf. The density of sea whips for the eastern Bering Sea averaged 0.11 ind. m^{-2}. In comparison, Miller et al. (2012) reported 0.24 ind. m^{-2} for Pribilof Canyon and 0.05 ind. m^{-2} for Zhemchug Canyon, and Brodeur (2001) reported densities in a grove of sea whips near Pribilof Canyon of 0.25 ind. m^{-2}. In other studies in Alaska, especially in the Gulf of Alaska, some areas of high sea whip density have also been observed, such as the sea whip grove in southeastern Alaska studied by Malecha & Stone (2009), with densities of ~0.5 ind. m^{-2}, and the maximum densities of *Protoptilum* sp. and *Halipteris willemoesi* near Kodiak found by Stone et al. (2005) of 16 and 6 ind. m^{-2}, respectively. The differences we found between the regions of the eastern Bering Sea are probably related to how much of the sandy habitat favored by sea whips is available.

The measured heights for corals, sponges and sea whips presented here are the first published for the eastern Bering Sea. Coral heights averaged 20 cm or less for most taxonomic groups. The exception was the bamboo corals, Isididae, which averaged about 48 ± 5.1 cm tall in the eastern Bering Sea. These taller corals occurred in deeper water on the slope to the north of Pribilof Canyon. Growth rates for Isididae indicate that large specimens of these species (>70 cm) are likely in excess of 50 yr old (Andrews et al. 2009). A single specimen from the Gulf of Alaska with a height of 120 cm (similar to the maximum height found during this study) was estimated to be 116 yr of age. There have been no aging studies for the other species of gorgonian corals observed during this study, but large red tree corals (~2 m tall) found in southeastern Alaska have been aged at over 100 yr old (Andrews et al. 2002). In the eastern Bering Sea, sponge height differed by group, as the hexactinellid sponges tended to be taller than the demosponges. Growth rates for these groups in temperate waters are not well known. Wilson et al. (2002) estimated a linear growth rate of 7.42 cm yr^{-1} for the interval between small (~27 cm) and medium (~100 cm) sea whips. Based on these growth rates, the average sized sea whip from the eastern Bering Sea (62 cm height) would be ~12 to 14 yr old.

Camera survey and model validation

Independent surveys to validate species distribution models are rarely undertaken. In most cases, model validation is performed by re-substitution (Kumar & Stohlgren 2009, Krigsman et al. 2012) or splitting the data set at random into training and testing data sets (Bryan & Metaxas 2007, Franklin et al. 2013, Sagarese et al. 2014). Using newly collected data that are independent of the original data set is less common, but usually utilizes data collected in additional years or additional areas (Eskildsen et al. 2013, Rooper et al. 2014). Using an independent data set collected with an entirely different survey design and data collection method is very rare (see Abecasis et al. 2014, Anderson et al. 2016 for exceptions), but it can provide the most insight into model performance (Elith et al. 2006).

The type of validation technique utilized can influence the perception of the model's predictive ability. In general, the more independent the cross-validation, the higher the chances that it will indicate problems in the original model. Because the GAM methodology used here can represent very complex

relationships between organisms and their environment, the GAMs are prone to over-fitting the data. We limited the number of inflection points ('knots') in the functional relationships in the GAMs, but this alone cannot entirely prevent model over-fitting. The support of the independent camera survey observations for the bottom trawl survey coral model provides confidence in the model predictions and an additional measure of the uncertainty around those predictions (Guisan et al. 2013).

We chose not to mix the 2 data sets (trawl and camera) when estimating combined models (e.g. combined coral model) because catchability, area swept, sample sizes and underlying survey design differed between the 2 surveys. Instead, combined models were created by averaging the predictions from each survey model; each combined model was a compromise fit to the 2 data sets (trawl and camera survey). Each individual data set best fitted its individual model, as expected. For example, for coral models, the AUC for the bottom trawl model predicting trawl data was 0.92 and the AUC for the camera model predicting the camera data was 0.95, whereas the cross-predictions yielded AUC of 0.73 (when the bottom trawl model predicted camera data and vice versa). The combined model fit resulted in AUCs of 0.85 and 0.90 for the trawl data and camera data, respectively. For coral, the combined model best matched both data sets, with a slightly better fit to the camera data than to the trawl data. The favorable matching of both data sets likely occurred because both individual coral models (trawl and camera) showed similar coral spatial distributions.

This is in contrast to the sponge model, where the 2 independent models and data sources did not agree as well. In this case, the combined model fitted both the camera and trawl data reasonably well (AUCs of 0.76 and 0.71, respectively), but not as well as for the coral model. This lack of coherence for the sponge models may have been due to the fact that the camera data did not cover shallow areas of the outer shelf, where there were trawl data. This implies that the sponge model is inadequate for extrapolating outside the camera survey area. Much of the disagreement between the camera and trawl models was on the northeast outer shelf, where the camera model predicted a high probability of sponge occurrence. Because the predicted probability of sponge presence increased with latitude and no camera sampling occurred in high-latitude shallow areas, these predictions represent extrapolation outside the camera survey area and thus are unreliable. The same phenomenon was also apparent with the sea whip predictions in the same area (northeastern outer shelf); these predictions also are unreliable.

Additionally, catchability for sponges may be higher in the trawl survey compared to the camera survey. Only sponges that exceeded 10 cm height were counted in the image analysis, since smaller specimens could not be identified from white- or yellow-colored items on the seafloor. However, some unknown fraction of these smaller sponges was caught by the trawl survey, thus contributing to the mismatch between the trawl and camera models. The opposite effect likely occurs for sea whips. All sea whips were easily observed and counted in the camera survey, but their trawl catchability likely is lower because of their flexibility (i.e. ability to bend without breaking off into the net), thus contributing to the mismatch between the camera and bottom trawl sea whip models.

CONCLUSIONS

The trawl-based model of coral presence or absence was generally accurate in predicting presence or absence in the camera survey. The trawl models were also accurate in predicting sponge and sea whip presence or absence, but to a lesser degree than for corals. The models that combined the trawl model predictions and camera model predictions also performed well. These combined model predictions reflected the distribution of corals, sponges and sea whips with better overall accuracy for both data sets (bottom trawl and camera) than the individual models did during cross-validation. For example, the combined sponge model performed better at predicting the camera observations of sponge than the trawl sponge model did at predicting the camera survey observations. Densities and heights of corals were generally highest in Pribilof Canyon and to the northwest of Pribilof Canyon along the slope. For sponges, densities and heights were highest surrounding Pribilof Canyon, north of Bering Canyon and in some locations in Zhemchug Canyon. Sea whip densities and heights were highest on the outer shelf between Pribilof and Zhemchug Canyon, and in an area to the south of Pribilof Canyon. Combining the trawl models and camera models showed improvement over models based on trawl data alone; the results demonstrate the benefit of independent data to evaluate species distribution model predictions for structure-forming invertebrates.

Acknowledgements. We thank Captain Tim Cosgrove and the crew of the FV 'Vesteraalen', and Steve MacLean for their assistance in completing the fieldwork. We thank Bob Stone, Jerry Hoff, Duane Stevenson and Jay Orr for their assistance in identifications of invertebrates and fishes. Megan Prescott assisted with the bathymetry data. Al Hermann provided ROMS model outputs for current speed and direction. The manuscript benefitted from reviews from Jerry Hoff, Jodi Pirtle, Wayne Palsson, David Somerton and 2 anonymous reviewers.

LITERATURE CITED

Abecasis D, Aronso P, Erzini K (2014) Combining multi-species home range and distribution models aids assessment of MPA effectiveness. Mar Ecol Prog Ser 513: 155–169

Anderson OF, Guinotte JM, Rowden AA, Clark MR, Mormedea S, Davies AJ, Bowden DA (2016) Field validation of habitat suitability models for vulnerable marine ecosystems in the South Pacific Ocean: implications for the use of broad-scale models in fisheries management. Ocean Coast Manage 120:110–126

Andrews AH, Cordes EE, Mahoney MM, Munk K, Coale KH, Cailliet GM, Heifetz J (2002) Age, growth and radiometric age validation of a deep-sea, habitat-forming gorgonian (*Primnoa resedaeformis*) from the Gulf of Alaska. Hydrobiologia 471:101–110

Andrews AH, Stone RP, Lundstrom CC, DeVogelaere AP (2009) Growth rate and age determination of bamboo corals from the northeastern Pacific Ocean using refined ^{210}Pb dating. Mar Ecol Prog Ser 397:173–185

Brodeur RD (2001) Habitat-specific distribution of Pacific Ocean perch (*Sebastes alutus*) in Pribilof Canyon, Bering Sea. Cont Shelf Res 21:207–224

Bryan TL, Metaxas A (2007) Predicting suitable habitat for deep-water gorgonian corals on the Atlantic and Pacific Continental Margins of North America. Mar Ecol Prog Ser 330:113–126

Coachman LK (1986) Circulation, water masses and fluxes on the southeastern Bering Sea shelf. Cont Shelf Res 5: 23–108

Cragg JG (1971) Some statistical models for limited dependent variables with application to the demand for durable goods. Econometrica 39:829–844

Davies AJ, Wisshak M, Orr JC, Roberts JM (2008) Predicting suitable habitat for the cold-water reef framework-forming coral *Lophelia pertusa* (Scleractinia). Deep-Sea Res I 55:1048–1062

Elith J, Graham CH, Anderson RP, Dudík M and others (2006) Novel methods improve prediction of species' distributions from occurrence data. Ecography 29:129–151

Engler R, Guisan A, Rechsteiner L (2004) An improved approach for predicting the distribution of rare and endangered species from occurrence and pseudo-absence data. J Appl Ecol 41:263–274

Eskildsen A, le Roux PC, Heikkinen RK, Høye TT and others (2013) Testing species distribution models across space and time: high latitude butterflies and recent warming. Glob Ecol Biogeogr 22:1293–1303

Franklin J, Davis FW, Ikegami M, Syphard AD, Flint LE, Flint AL, Hannah L (2013) Modeling plant species distributions under future climates: How fine scale do climate projections need to be? Global Change Biol 19:473–483

Guinotte JM, Davies AJ (2014) Predicted deep-sea coral habitat suitability for the U.S. west coast. PLoS ONE 9: e93918

Guisan A, Tingley R, Baumgartner JB, Naujokaitis-Lewis I, Sutcliffe PR (2013) Predicting species distributions for conservation decisions. Ecol Lett 16:1424–1435

Howell KL, Holt R, Endrino IP, Stewart H (2011) When the species is also a habitat: comparing the predictively modelled distributions of *Lophelia pertusa* and the reef habitat it forms. Biol Conserv 144:2656–2665

Kaplan IC, Williams GD, Bond NA, Hermann AJ, Siedlecki SA (2016) Cloudy with a chance of sardines: forecasting sardine distributions using regional climate models. Fish Oceanogr 25:15–27

Krigsman LM, Yoklavich MM, Dick EJ, Cochrane GR (2012) Models and maps: predicting the distribution of corals and other macro-invertebrates in shelf habitats. Ecosphere 3:1–16

Kumar S, Stohlgren TJ (2009) Maxent modeling for predicting suitable habitat for threatened and endangered tree *Canacomyrica monticola* in New Caledonia. J Ecol Nat Environ 1:94–98

Leverette TL, Metaxas A (2005) Predicting habitat for two species of deep-water coral on the Canadian Atlantic continental shelf and slope. In: Freiwald A, Roberts JM (eds) Cold-water corals and ecosystems. Springer-Verlag, Berlin, p 467–479

Malecha PW, Stone RP (2009) Response of the sea whip *Halipteris willemoesi* to simulated trawl disturbance and its vulnerability to subsequent predation. Mar Ecol Prog Ser 388:197–206

Miller RJ, Hocevar J, Stone RP, Fedorov DV (2012) Structure-forming corals and sponges and their use as fish habitat in Bering Sea submarine canyons. PLoS ONE 7: e33885

Miller RJ, Juska C, Hocevar J (2015) Submarine canyons as coral and sponge habitat on the eastern Bering Sea slope. Glob Ecol Conserv 4:85–94

Potts J, Elith J (2006) Comparing species abundance models. Ecol Modell 199:153–163

R Development Core Team (2013) R: a language and environment for statistical computing. R Foundation for Statistical Computing, Vienna. www.R-project.org

Rengstorf AM, Yesson C, Brown C, Grehan AJ (2013) High-resolution habitat suitability modelling can improve conservation of vulnerable marine ecosystems in the deep sea. J Biogeogr 40:1702–1714

Rooper CN, Zimmermann M, Prescott MM, Hermann AJ (2014) Predictive models of coral and sponge distribution, abundance and diversity in bottom trawl surveys of the Aleutian Islands, Alaska. Mar Ecol Prog Ser 503: 157–176

Sagarese SR, Frisk MG, Cerrato RM, Sosebee KA, Musick JA, Rago PJ (2014) Application of generalized additive models to examine ontogenetic and seasonal distributions of spiny dogfish (*Squalus acanthias*) in the northeast (US) shelf large marine ecosystem. Can J Fish Aquat Sci 71:847–877

Sigler MF, Rooper CN, Hoff GR, Stone RP, McConnaughey RA, Wilderbuer TK (2015) Faunal features of submarine canyons on the eastern Bering Sea slope. Mar Ecol Prog Ser 526:21–40

Springer AM, McRoy CP, Flint MV (1996) The Bering Sea Green Belt: shelf-edge processes and ecosystem production. Fish Oceanogr 5:205–223

Stein DL, Tissot BN, Hixon MA, Barss W (1992) Fish-habitat associations on a deep reef at the edge of the Oregon continental shelf. Fish Bull 90:540–551

Stone RP (2006) Coral habitat in the Aleutian Islands of Alaska: depth distribution, fine-scale species associations, and fisheries interactions. Coral Reefs 25:229–238

Stone RP (2014) The ecology of deep-sea coral and sponge habitats of the central Aleutian Islands of Alaska. NOAA Prof Paper NMFS 16. US Department of Commerce, Seattle, WA

Stone RP, Masuda MM, Malecha PW (2005) Effects of bottom trawling on soft-sediment epibenthic communities in the Gulf of Alaska. In: Barnes PW, Thomas JP (eds) Benthic habitats and the effects of fishing. Am Fish Soc Symp 41, Bethesda, MD, p 461–475

Stone RP, Lehnert H, Reiswig H (2011) A guide to the deep-water sponges of the Aleutian Island Archipelago. NOAA Prof Paper NMFS 12. US Department of Commerce, Seattle, WA

Taylor ML, Yesson C, Agnew DJ, Mitchell RE, Rogers AD (2013) Using fisheries by-catch data to predict octocoral habitat suitability around South Georgia. J Biogeogr 40: 1688–1701

Voorhees D, Lowther A (2012) Current fishery statistics no. 2011. National Marine Fisheries Service, Silver Spring, MD

Wiens JA, Stralberg D, Jongsomjit D, Howell CA, Snyder MA (2009) Niches, models, and climate change: assessing the assumptions and uncertainties. Proc Natl Acad Sci USA 106:19729–19736

Williams K, Rooper CN, Towler R (2010) Use of stereo camera systems for assessment of rockfish abundance in untrawlable areas and for recording pollock behavior during midwater trawls. Fish Bull 108:352–362

Wilson MT, Andrews AH, Brown AL, Cordes EE (2002) Axial rod growth and age estimation of the sea pen, *Halipteris willemoesi* Kölliker. Hydrobiologia 471:133–142

Wood SN (2006) Generalized additive models: an introduction with R. Chapman & Hall, Boca Raton, FL

Woodby D, Carlile D, Hurlburt L (2009) Predictive modeling of coral distribution in the Central Aleutian Islands, USA. Mar Ecol Prog Ser 397:227–240

Yoklavich MM, Greene HG, Cailliet GM, Sullivan DE, Lea RN, Love MS (2000) Habitat associations of deep-water rockfishes in a submarine canyon: an example of a natural refuge. Fish Bull 98:625–641

Editorial responsibility: Romuald Lipcius, Gloucester Point, Virginia, USA

Submitted: October 8, 2015; Accepted: March 20, 2016
Proofs received from author(s): May 24, 2016